Title: The Feedback-Related Negativity (FRN) Sig-nals Strategic Adaptation in Hierarchical De-cision-Making: An EEG Investigation

Authors: Leyla Yahyaie[1], Reza Ebrahimpour[2,*],

1. *Islamic Azad University, Salamas Branch, Salamas, Iran.*
2. *Sharif University, Tehran, Iran.*

***Corresponding Author**: Reza Ebrahimpour, Sharif University, Tehran, Iran. Email: ebrahimpour@sharif.edu

To appear in: **Basic and Clinical Neuroscience**

Received date: 2024/08/08

Revised date: 2026/02/02

Accepted date: 2026/02/03

Please cite this article as:

Yahyaie, L., Reza Ebrahimpour, R. (In Press). The Feedback-Related Negativity (FRN) Sig-nals Strategic Adaptation in Hierarchical De-cision-Making: An EEG Investigation. Basic and Clinical Neuroscience. Just Accepted publication Jul. 10, 2026. Doi: http://dx.doi.org/10.32598/bcn.2026.276.4

DOI: http://dx.doi.org/10.32598/bcn.2026.276.4

Abstract

Background: Electroencephalogram (EEG) signals, which measure the brain's electrical activity, are known to encode information about low-level perceptual decision-making. However, whether these signals also reflect hierarchical decision-making processes—wherein high-level decisions depend on the outcomes of low-level decisions and prior decision history—remains unclear. The accuracy of this integrated process is guided by feedback. Since negative feedback can result from errors at the low level, high level, or both, its precise source is often ambiguous.

Objective: This study aimed to determine whether feedback-related negativity (FRN) derived from EEG signals reflects the dynamics of hierarchical decision-making.

Methods: Participants performed a hierarchical decision-making task while EEG signals were recorded, and they reported both low- and high-level decisions simultaneously via saccadic eye movements toward a single target. Correct feedback was delivered only when both decisions were accurate. The FRN component was analyzed at electrodes F3, F4, Fz, and Cz.

Results: The FRN component conveyed information about hierarchical decisions, with amplitude increasing significantly during consecutive negative feedback trials and prior to changes in high-level decision strategy.

Conclusions: These findings suggest that brain activity underlying hierarchical decision-making modulates the FRN component.

Keywords: Hierarchical decision-making; Confidence; EEG signals; Strategy updating; feedback-related negativity

EEG=Electroencephalogram. FRN=Feedback-Related Negativity. ACC=Anterior Cingulate Cortex. RDM=Random Dot Motion. ICA=Independent Component Analysis. DMFC=Dorsal Medial Frontal Cortex.

Introduction

Real-world decisions are rarely made in isolation. Instead, they are often embedded within hierarchical structures, where rapid, perceptual choices are guided by slower, strategic assessments of the broader context (Knudsen et al., 2018; Sarafyazd & Jazayeri, 2019). This interplay between different levels of processing is fundamental to adaptive behavior, allowing organisms to flexibly update their strategies based on experience. Pioneering work has formalized this hierarchy using computational models and behavioral tasks (Purcell & Kiani, 2016), identifying three core parameters that drive high-level strategic updates: (1) confidence in low-level perceptual decisions, (2) the history of consecutive errors, and (3) decision urgency (Miletić, 2016; Purcell & Kiani, 2016; Sarafyazd & Jazayeri, 2019). A key challenge in cognitive neuroscience is to uncover how the human brain dynamically integrates these distinct sources of information to govern behavioral change (Azizi & Ebrahimpour, 2023; Ghaderi-Kangavar et al., 2023; Roshan et al., 2024).

The feedback-related negativity (FRN), a frontocentral event-related potential (ERP) peaking 200–300 ms after feedback onset, is a prime candidate for probing these neural computations (Li & Zhou, 2017; Nieuwenhuis et al., 2004). The FRN is consistently elicited by feedback indicating errors or the omission of expected rewards (negative feedback and reward prediction errors), marking it as a neural signal deeply involved in outcome evaluation and learning (Holroyd & Coles, 2002; Valladares et al., 2017; Salami et al., 2022). Its typical frontal-central scalp distribution suggests an association with theta-band activity in the medial frontal cortex, and it is linked to rapid feedback evaluation and dopaminergic shifts between the basal ganglia and anterior cingulate cortex (ACC) (Lim et al., 2018; Rawls et al., 2020; Wang et al., 2020b; Zhong et al., 2020). Critically, the FRN's amplitude is not a monolithic response; it is thought to reflect a

discrepancy between reward and punishment signals (a prediction error) and is modulated by several factors relevant to hierarchical control (Gupta & Deák, 2015; Parashiva & Vinod, 2021). For instance, the FRN is sensitive to reward magnitude (e.g., larger for monetary losses than gains), is influenced by post-decision confidence, and reflects individual differences in executive functions and risk-taking propensity (e.g., in methamphetamine dependence) (Boldt & Yeung, 2015; Lim et al., 2018; Zottoli & Grose-Fifer, 2012; Zhong et al., 2020). This confluence of properties—sensitivity to feedback, link to learning, and modulation by confidence and control—suggests that the FRN may serve as a real-time neural index that aggregates low-level decision variables to inform high-level strategic shifts (Zizlsperger et al., 2014).

However, a critical gap remains. While the FRN's links to basic feedback processing and isolated cognitive constructs are well-established, it is unknown whether it systematically tracks the specific, interacting parameters posited by hierarchical decision-making models—namely, low-level confidence (inferable from stimulus strength), error history, and decision urgency—within a single, unified paradigm (Peixoto et al., 2021; Murphy et al., 2021). Does the FRN amplitude scale with the accumulation of consecutive negative evidence? Does it signal the growing urgency to abandon a failing strategy? In short, can the FRN be understood not just as a marker of feedback valence, but as a reflection of the dynamic computations underlying hierarchical behavioral adaptation?

To address these questions, we employed a well-established hierarchical decision-making task (Purcell & Kiani, 2016) while recording electroencephalography (EEG) in human participants. This paradigm requires observers to simultaneously make a low-level perceptual decision (discriminating the direction of random dot motion, RDM) and a high-level strategic decision (inferring the current environmental state) (von Lautz et al., 2019). The brain commits to such

decisions once accumulated sensory evidence reaches a critical threshold (Iribe-Burgos et al., 2022; García-Hernández et al., 2022; McCracken et al., 2020; Shooshtari et al., 2019; Yahyaie et al., 2024), and feedback is crucial for adapting future behavior (Sarafyazd & Jazayeri, 2019). We analyzed the FRN to test our central hypothesis: that its amplitude would be selectively modulated by the three key hierarchical parameters. Specifically, we predicted that FRN amplitude would (1) increase with the accumulation of consecutive negative feedback, (2) be larger for errors occurring under high decision urgency (just before a strategy switch), and (3) show sensitivity to the strength of sensory evidence (motion coherence), a proxy for low-level decision confidence. Our findings confirm these predictions, demonstrating that the FRN is a sensitive neural correlate of the multi-faceted computational processes that guide hierarchical decision-making and strategic behavioral updates.

METHODS

Participants

Our study involved twenty-one subjects (12 females, all right-handed, aged between 25 and 38) in a hierarchical decision-making task, selected from diverse backgrounds to capture a broad spectrum of perspectives. Upon analysis, significant noise was detected in the EEG data from two subjects, leading to their exclusion from the study's analysis. The ethics committee of the Iran University of Medical Sciences provided approval for the experiment (Ethics ID IR.IUMS.REC.1399.1081), and all subjects furnished informed written consent before commencement. None of the subjects had a history of psychiatric or neurological disorders. Additionally, each subject boasted normal or corrected-to-normal vision. Before the experiment, detailed instructions were provided to the subjects in written form. Following this, subjects

engaged in a test block comprising 200 trials. Their performance in discerning the direction of random dot motion (RDM) task presented on a computer screen was assessed, and they were subsequently assigned an accuracy score. Training on the fundamental motion discrimination task persisted until subjects achieved proficient performance, manifested by psychophysical thresholds of less than 17% (roughly 80% accuracy in indicating the correct direction of random dots motion within a test block).

Procedure

Before the main experiment, subjects underwent a training phase, including a simple random dot motion (RDM) task (Figure 1A), where they had to identify the direction of coherent motion within a grid of randomly moving dots. The task's difficulty was modulated by adjusting the coherence level, representing the strength of the stimulus or motion coherence. Figure 1B illustrates the random dot kinematogram (RDK) stimulus employed in the RDM experiment, featuring a field of dots, with a certain percentage moving coherently in one direction (signal dots), while the remainder moved randomly (noise dots). Various coherence levels were depicted, with higher coherence indicating a larger proportion of signal dots, facilitating easier perception of motion direction (Newsome and Pare, 1988). The experiment utilized the Psychophysics Toolbox and Matlab for stimulus control, with EyeLink by SR-Research tracking eye movements.

The training trial structure was as follows: Each trial began with the subject fixating on a small red circle (0.3° diameter) at the screen center. After a delay (200-500 ms; truncated exponential), two red targets (0.5°) appeared equidistant from the fixation point (8° eccentricity). Subsequently, a dynamic random dots stimulus appeared within a 5° circular aperture centered on the fixation point after another random delay (200-500 ms; truncated exponential). The dots were white 4x4-pixel squares (0.096° x 0.096°) on a black background, with a density of 16.7 dots per square degree per

second (Figure 1A). After the motion stimulus offset, a delay period (400-1000 ms; truncated exponential) preceded the fixation point offset. Subjects were instructed to maintain gaze on the fixation point until its offset. Deviation exceeding 2° aborted the trial. Subjects reported the perceived motion direction by shifting gaze to the chosen target and maintaining gaze within 3° for 200 ms. Correct responses received positive feedback, while incorrect responses received negative feedback. The RDM task has been introduced in a previous study (Shadlen and Newsome, 2001). The training continued until subjects achieved high performance (thresholds <17%).

The main experiment focused on simultaneous low- and high-level decision-making, depicted in Figure 1C. Following motion direction discrimination training, subjects transitioned to the changing environment task (Figure 1C). The experimental setup, motion stimulus, and event timing were consistent with the training protocol, but subjects were presented with two pairs of choice targets (four targets total) positioned above and below the fixation point (FP) at 10° eccentricities (±3.5° above/below FP; ±9.4° left/right of FP). Each pair of targets represented right and left motion directions, with the upper and lower pairs indicating two distinct environments. For example, selecting the top-left target (Figure 1C) indicated recognition of leftward dot motion and an upward environmental orientation.

The hierarchical task paradigm began with a small red fixation point at the screen's center (Figure 1C). Subjects were required to focus on the red fixation point for approximately 200 ms, and if their gaze deviated by more than 2°, the trial was aborted. Following a random delay (ranging from 200 to 500 ms, obtained from a truncated exponential distribution), two pairs of targets appeared on the screen. The horizontal targets indicated the environmental orientation—whether upward or downward (Figure 1C). After an additional random delay (again ranging from 200 to 500 ms, obtained from a truncated exponential distribution), dot motion ensued. The duration of dot motion

varied randomly, selected from a truncated exponential distribution (ranging from 100 to 900 ms with a mean of 330 ms) for each trial. According to a truncated geometric distribution, the environment remained constant for several trials (ranging from 2 to 15 trials with a mean of 6). At intervals, without warning, the environment changed, prompting subjects to adjust their strategies. Subjects reported their responses— including the direction of random dot motion, and the environment by fixating on one of the targets and maintaining their gaze for 200 ms using saccadic eye data. This report was based on the history of feedback, choice, and confidence of choice related to several prior trials. Subjects received feedback following the announcement of their decision. Two audible tones were utilized to communicate decision feedback to the subjects, with 250 Hz denoting a correct answer and 1000 Hz indicating an incorrect one. Positive feedback was given when both low- and high-level decisions were correct; negative feedback was given otherwise. In both training phase and main experiment, the dot motion featured six different coherence levels (0%, 3.2%, 6.4%, 12.8%, 25.6%, 51.2%), and trials featuring 0% coherence were randomly selected from a uniform distribution for their motion direction. The experimental paradigm was inspired by previous work (Purcell and Kiani, 2016a). Each subject went through 4 to 8 blocks in a session, with each block comprising 200 trials. Out of 16800 trials,1100 trials were excluded

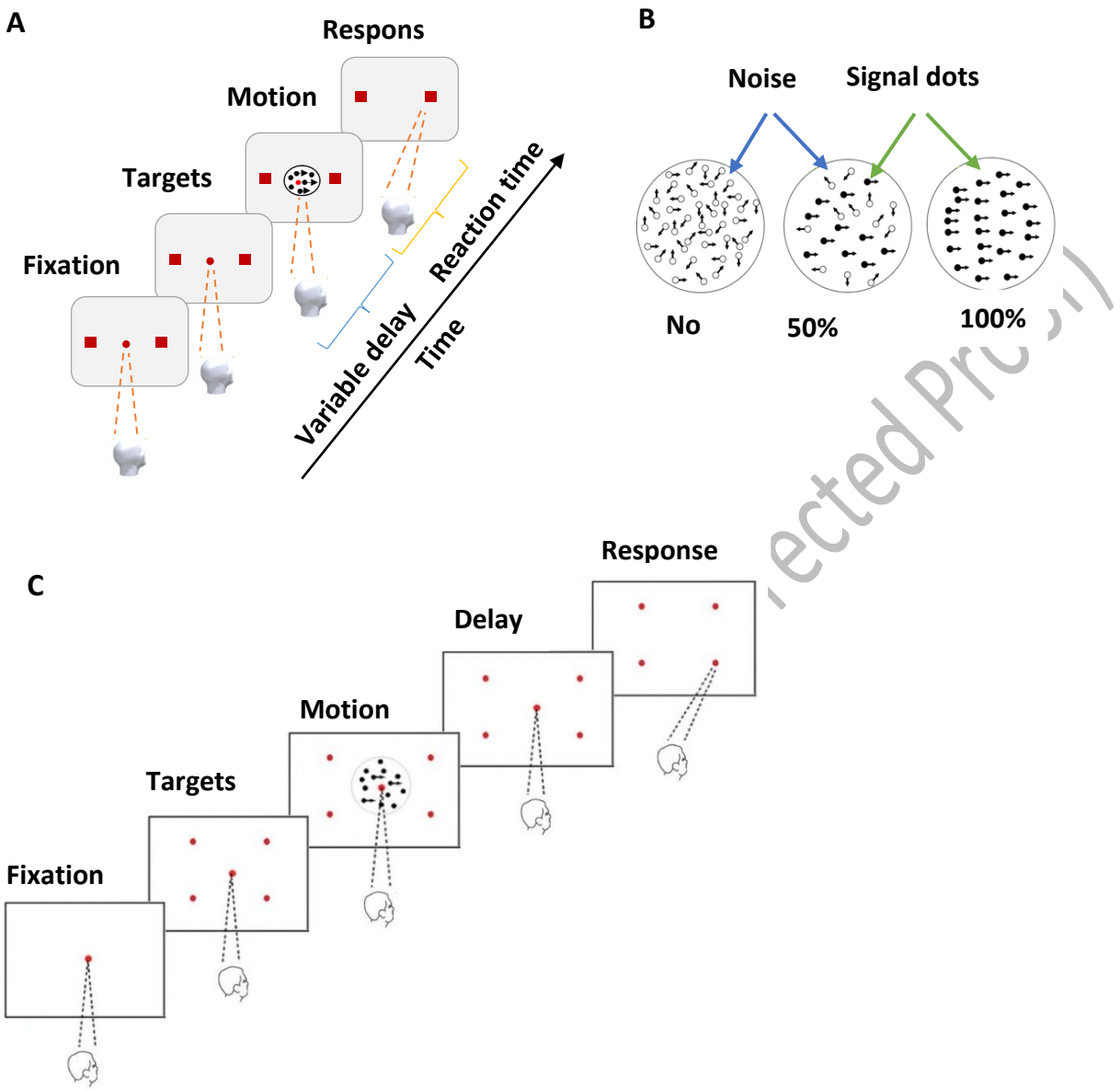

Figure 1. Experimental design and hierarchical decision-making task. (A)

Trial structure of the initial Random Dot Motion (RDM) training task. Each trial began with central fixation, followed by the presentation of two choice targets. A random-dot motion stimulus was then displayed within a central aperture, and participants reported the perceived direction of coherent motion by making a saccade to the corresponding target. Auditory feedback was provided

after the response. **(B)** Schematic representation of the Random Dot Kinematogram (RDK) stimulus. The stimulus consisted of a field of dots in which a variable percentage (coherence) moved coherently in one direction (signal dots, indicated by arrows), while the remaining dots moved randomly (noise dots). Higher coherence levels facilitate motion discrimination. **(C)** Structure of the main hierarchical decision-making task. Two pairs of choice targets (four targets total) were presented above and below the fixation point, corresponding to two possible environmental states (e.g., "Up" and "Down" environments). Within each environment, the left and right targets represented the two possible motion directions (e.g., leftward vs. rightward). Participants simultaneously reported both their low-level decision (motion direction) and high-level decision (inferred environment) with a single saccade to one of the four targets. Correct feedback was given only when both decisions were accurate. The task required participants to track feedback history to infer the currently active environment and adjust their strategy when necessary.

Recording, Preprocessing, and Analysis of EEG Signals

Electroencephalographic (EEG) data were recorded concurrently with eye tracking throughout the experiment. Participants were seated in a semi-darkened, electrically shielded room at a viewing distance of 57 cm from a 17-inch CRT monitor (PF790; 75 Hz refresh rate, 800 × 600 resolution). Continuous EEG was acquired using a 32-channel amplifier (eWave, Science Beam) from 31 scalp electrodes positioned according to the international 10–20 system (Fp1, Fp2, F3, F4, C3, C4, P3, P4, O1, O2, F7, F8, T3, T4, T5, T6, Fz, Cz, Pz, FC3, FC4, CP3, CP4, FT7, FT8, TP7, TP8, Oz). Signals were referenced online to the right mastoid, with the left mastoid serving as ground. Data were sampled at 1000 Hz, and electrode impedances were kept below 10 kΩ.

Offline preprocessing was performed using EEGLAB and custom MATLAB scripts. Continuous data were band-pass filtered between 0.1 and 35 Hz using a zero-phase Butterworth filter, followed by a 50 Hz notch filter to remove line noise. Ocular and muscular artifacts were corrected using Independent Component Analysis (ICA) with the ADJUST plugin for automatic component classification (Mognon et al., 2011). Bad channels were identified by visual inspection and interpolated using spherical spline interpolation.

For FRN analysis, the cleaned EEG data were segmented into epochs time-locked to feedback onset, spanning from −100 to 500 ms. Baseline correction was applied using the −100 to 0 ms pre-feedback interval. Epochs containing residual artifacts exceeding ±100 μV were automatically rejected.

To characterize the temporal dynamics of the FRN, the post-feedback interval was divided into consecutive, non-overlapping 100-ms windows (0–100, 100–200, 200–300, 300–400, and 400–500 ms). Within each window, the mean ERP amplitude at frontocentral electrodes was computed and statistically compared across experimental conditions using the Kruskal–Wallis test. The FRN was operationally defined as the mean amplitude within the time window exhibiting the strongest negative deflection and significant condition effects. The peak latency of the FRN was identified within this window for descriptive purposes only.

FRN amplitudes were quantified at a cluster of frontocentral electrodes (F3, F4, Fz, Cz), consistent with the canonical scalp distribution of this component (Pfabigan et al., 2015; Wang et al., 2020a). For each participant and experimental condition, FRN amplitude was calculated by averaging across all valid trials. Grand-averaged ERP waveforms revealed a robust negative deflection following negative feedback, replicating the characteristic morphology of the FRN (Oliveira et al.,

2005; Wang et al., 2020a) and supporting the validity of the preprocessing and analysis pipeline. All statistical analyses were conducted in MATLAB (R2021b).

Statistical analysis

All statistical analyses were conducted in MATLAB (R2021b, MathWorks Inc.). The Shapiro-Wilk test was used to assess normality, and as most behavioral and electrophysiological data violated this assumption ($p < 0.05$), non-parametric tests were employed throughout. Data are presented as mean ± standard error of the mean (SEM), and effect sizes are reported for all significant results. For behavioral analyses examining the effects of stimulus coherence and feedback history on strategy switching, the Kruskal-Wallis H-test was used for comparisons across three or more conditions (e.g., switching probability after 1, 2, or 3 consecutive errors), with significant main effects followed by Dunn's post-hoc tests and Bonferroni correction. Paired comparisons (e.g., switching after negative vs. positive feedback) were performed using the Wilcoxon signed-rank test. For electrophysiological data, FRN amplitude was analyzed according to our three primary hypotheses. The effect of stimulus strength was tested by comparing FRN amplitudes between high- and low-coherence negative feedback trials using a Wilcoxon rank-sum test. The effect of consecutive negative feedback was assessed by comparing FRN amplitudes following the first, second, and third consecutive errors (pre-switch) with the Kruskal-Wallis H-test and Dunn's post-hoc tests. The effect of decision urgency was evaluated by comparing FRN amplitudes from trials categorized by their proximity to a strategy switch (Distant: 7–9 trials before; Intermediate: 4–6 before; Immediate: 1–3 before) using the Kruskal-Wallis H-test and Dunn's post-hoc tests. Additionally, a Wilcoxon signed-rank test was used to compare FRN amplitude in the trial immediately preceding a switch to the trial immediately following it. For all

EEG analyses involving multiple comparisons, p-values were adjusted using the False Discovery Rate (FDR) correction (Benjamini-Hochberg procedure, $\alpha = 0.05$), and all reported FRN p-values are FDR-corrected. Functional connectivity, analyzed via Pearson correlation between electrode time-series in the FRN window, was compared across conditions for key electrode pairs (e.g., Fz–Cz) using Wilcoxon signed-rank tests with FDR correction. Effect sizes are reported as eta-squared (η^2) for Kruskal-Wallis tests and rank-biserial correlation (r) for Wilcoxon tests. All tests were two-tailed, with significance set at $p < 0.05$ after FDR correction where applicable.

RESULTS

Behavioral data analysis

We first examined the behavioral data to determine how the three key parameters of hierarchical decision-making—stimulus strength (a proxy for low-level confidence), the sequence of consecutive negative feedbacks, and decision urgency—guide strategic switching in a dynamic environment. Our results align with established findings (Purcell & Kiani, 2016a), confirming the validity of our experimental approach.

Initial analyses focused on the psychophysical properties of the task. Consistent with known principles, perceptual accuracy improved as stimulus strength (coherence) increased. This relationship was formalized by fitting a cumulative Weibull function to the choice data (Quick, 1974), providing psychophysical thresholds (α) and slopes (β) for each participant (Figure 2A; Palmer et al., 2005; Zylberberg et al., 2016).

The core of the behavioral analysis addressed how feedback drives strategy updates. Following positive feedback, participants almost always maintained their current environmental strategy (Figure 2B, light-blue line). Conversely, negative feedback robustly elicited strategy switches,

with a greater likelihood of switching when errors occurred under high stimulus strength (Figure 2B, red line). Because negative feedback could result from either a low-level (motion) or high-level (environment) error, participants often needed to accumulate evidence across trials to identify the source. Accordingly, the probability of switching grew with the number of consecutive negative feedbacks (Figure 2C). This relationship was modulated by stimulus strength: switches were most probable when strong sensory evidence (high coherence) converged with repeated negative outcomes, implying increased certainty that the high-level strategy was incorrect (Figure 2D; Kruskal-Wallis test, $H(2) = 9.97$, $p = 0.007$; Purcell & Kiani, 2016a; Sarafyazd & Jazayeri, 2019).

Finally, we assessed the influence of decision urgency. The tendency to switch after negative feedback also rose with the duration spent in the same environment (Figure 2E), suggesting that elapsed time—an indicator of mounting decision urgency—can itself trigger a strategic shift, independent of immediate feedback. Moreover, the interaction between stimulus strength and environmental history significantly shaped switching probability (Figure 2F; Kruskal-Wallis test, $H(2) = 13.58$, $p = 0.004$). As a control check, strategy switches were exceedingly rare after positive feedback (Figure 2H), underscoring that behavioral adaptation was principally governed by negative outcomes.

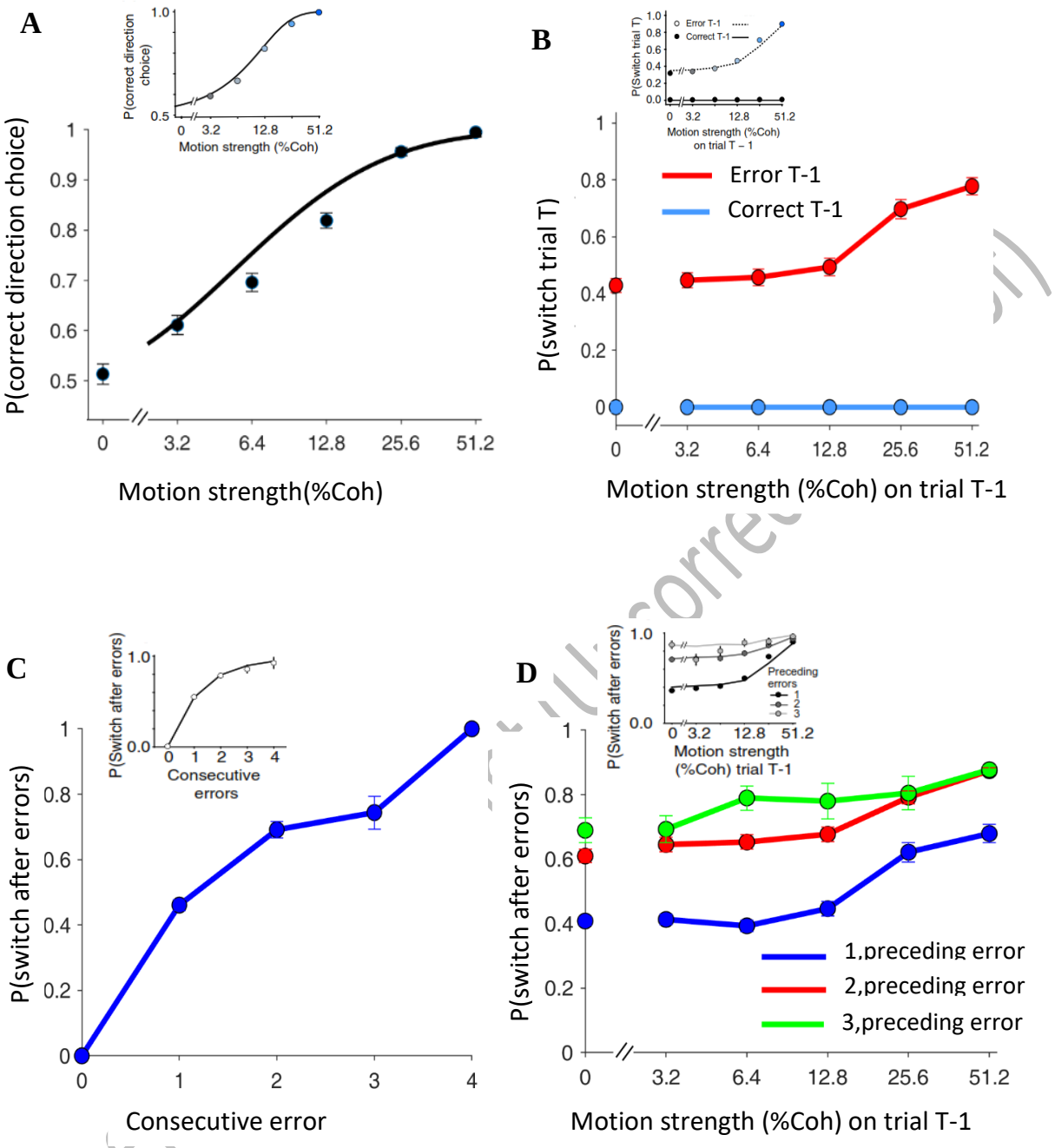

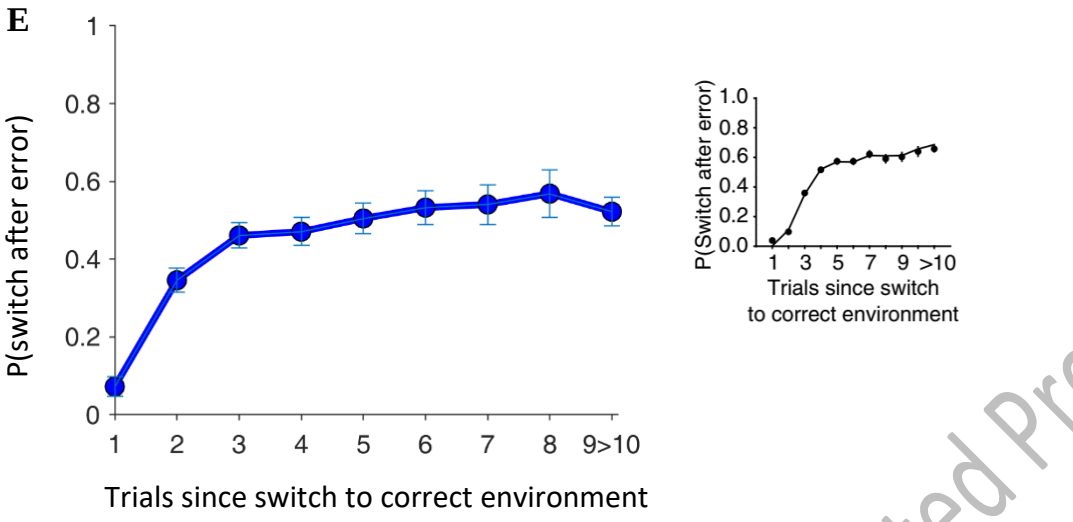

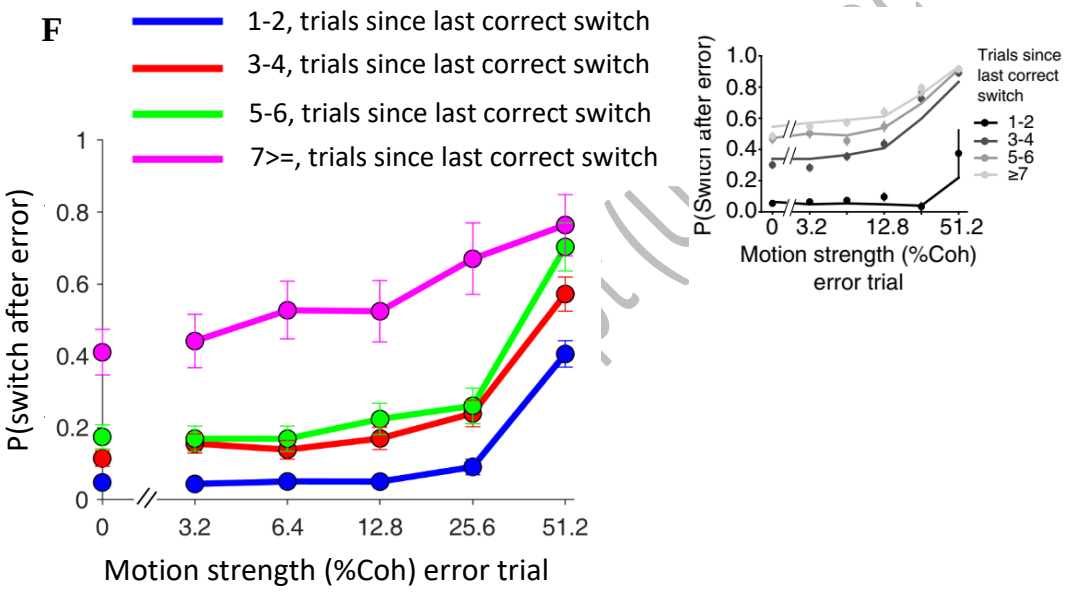

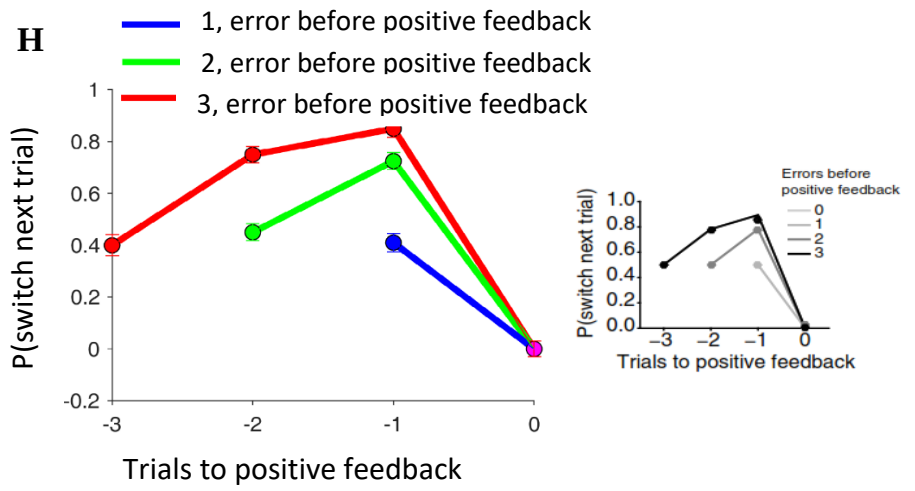

Figure 2. Behavioral results: Psychometric function and strategy switching probabilities. (A)

Psychometric function relating motion coherence to perceptual accuracy. Data points represent mean accuracy (±SEM), fitted with a cumulative Weibull function (threshold $\alpha = 0.8352$; slope $\beta = 5.0578$). Accuracy increases with coherence, and variability decreases at higher coherence levels. **(B)** Probability of switching the high-level strategy (environment) following positive vs. negative feedback, plotted as a function of motion coherence. Positive feedback (blue) leads to stable strategy maintenance, whereas negative feedback (red) prompts switching, especially when motion strength is high. **(C)** Switch probability increases with the number of consecutive negative feedbacks, reflecting evidence accumulation for a strategy change. **(D)** Combined influence of motion coherence (stimulus strength) and consecutive negative feedback count on switch probability. Warmer colors indicate a higher number of consecutive errors. Switching is most likely when strong sensory evidence coincides with repeated negative outcomes. **(E)** Switch probability following negative feedback as a function of trials elapsed since the last correct strategy change. Longer periods in the same environment increase switching tendency, a marker of growing decision urgency. **(F)** Interaction between motion coherence and environmental history (trials since last change) in modulating switch probability after negative feedback. **(G)** As a control, switch probability following positive feedback is near zero across all conditions, confirming that strategy updates are driven primarily

by negative outcomes. In all panels, symbols show group mean ± SEM. Gray insets in B, C, D are adapted from Purcell & Kiani (2016a) and Sarafyazd & Jazayeri (2019) for comparison.

FRN Amplification Scales with High-Low Level Stimulus Features

To examine whether the Feedback-Related Negativity (FRN) is sensitive to low-level perceptual features, we compared its amplitude on negative feedback trials as a function of stimulus clarity. Trials were categorized into two groups based on motion coherence: high stimulus strength (coherence: 12.8%, 25.6%, 51.2%) and low stimulus strength (coherence: 3.2%, 6.4%). Analysis of the mean FRN amplitude in the post-feedback window revealed a significantly larger (more negative) response following negative feedback in high-strength compared to low-strength trials (Figure 3, Wilcoxon signed-rank, $p < 0.05$;).

This result indicates that the FRN is modulated not only by high-level decision errors but also by the quality of the sensory evidence. Notably, larger FRN amplitudes were elicited by negative feedback when the stimulus was clearer and the probability of a low-level perceptual error was reduced. This pattern is consistent with prior work showing that the strength of sensory evidence modulates neural signals involved in performance monitoring, such as the centroparietal positivity (CPP; Kelly & O'Connell, 2013).

Taken together, these findings suggest that the FRN serves as a neural index that integrates both low-level and high-level decision parameters. It reflects not only the presence of an error but also the certainty associated with the perceptual decision (lower uncertainty with higher coherence) and the resulting instructional value of the feedback for updating behavior. This integrated view positions the FRN as a marker of hierarchical evidence processing, linking sensory certainty to adaptive decision-making in dynamic environments.

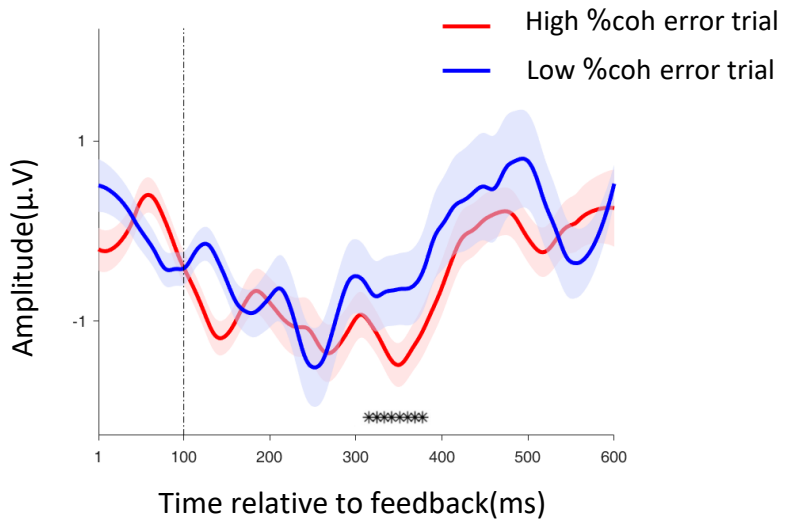

Figure 3. Feedback-Related Negativity (FRN) amplitude modulated by stimulus coherence.

The grand-average event-related potential (ERP) waveforms, time-locked to negative feedback, are plotted separately for trials with high stimulus strength and low stimulus strength. The region marked with an asterisk (*) indicates the FRN time window (100–500 ms post-feedback), within which the FRN amplitude was significantly larger (more negative) for high stimulus strength trials (Wilcoxon signed-rank, $p < 0.05$). The shaded areas represent the standard error of the mean (SEM).

FRN Amplification Scales with Consecutive Negative Feedback

In the pre-switch trials (i.e., the trial immediately preceding each environmental change), we conducted an in-depth examination of three consecutive negative feedback signals. The pre-switch trials were initially categorized into three distinct groups based on the sequence of negative feedback: (1) first successive negative feedback instance, (2) second successive negative feedback instance, and (3) third successive negative feedback instance. The first category consisted of trials where participants received negative feedback in the current trial and subsequently switched to another environment in the next trial(s). The second category included trials where participants received negative feedback in two consecutive trials (the current and the previous trial) before

switching environments. The third category comprised trials where participants received negative feedback across three consecutive trials prior to switching.

The occurrence of negative feedback indicates that a decision was either erroneous at a low level (an incorrect perceptual response) or misjudged at a high level (an incorrect environment selection). In both cases, the specific cause of the negative feedback remained ambiguous, which likely prompted participants to actively seek additional information across trials. Notably, as information accumulated, the amplitude of the FRN signal exhibited a corresponding increase, aligned with the frequency of negative feedback instances.

Our findings revealed a significant discrepancy in FRN amplitude following successive negative feedback. As negative feedback accumulated, FRN amplitude demonstrated a corresponding increase that aligned with feedback frequency. Statistical analysis confirmed a significant difference in FRN amplitude across the three conditions (Figure 4A; Kruskal-Wallis Test, $p < 0.05$). Post-hoc comparisons indicated that the amplitude in the third condition was significantly larger than both the first ($p < 0.008$) and second ($p < 0.021$) conditions. The difference between the first and second conditions showed a non-significant trend ($p < 0.052$). Mean FRN amplitudes (±SEM) were: first: -2.1 ± 0.5 μV; second: -2.8 ± 0.6 μV; third: -3.6 ± 0.7 μV.

Additionally, topography analysis further corroborated this outcome. By evaluating the signal amplitudes concerning a reference (the right mastoid), a brain topography depiction was generated utilizing a color spectrum ranging from red to blue. This map effectively delineated the activity of the frontal and central-parietal areas during three consecutive negative feedback instances (Figure 4B).

To further investigate functional interactions between brain regions, we conducted connectivity analysis to examine correlations among EEG signals across the three consecutive negative

feedback conditions (one, two, and three instances). This analysis allowed us to assess how different cortical areas coordinated their activity in response to accumulating feedback. Following established methodology (Barzegaran & Knyazeva, 2017), we analyzed signals from all 29 EEG channels involved in hierarchical decision-making.

Consistent with expectation, within-channel correlations (i.e., a channel correlated with itself) were highest. Notably, our connectivity assessment identified F3, F4, Fz, and Cz as the most strongly interrelated channels across conditions. This pattern underscores the central role of frontal and central midline regions in processing sequential negative feedback.

We focused our correlation-based connectivity analysis on the post-feedback window, corresponding to the typical FRN peak. The resulting connectivity matrices (Figure 4C, D, E) demonstrated a systematic increase in correlation strength with successive negative feedback. Quantitatively, the correlation between the Fz and Cz electrodes increased progressively: first negative feedback: $r=0.43 \pm 0.09$; second: $r=0.49 \pm 0.15$; third: $r=0.58 \pm 0.16$.

Statistical comparison of these correlation values confirmed that connectivity following three consecutive negative feedback instances was significantly stronger than after a single instance ($p = 0.035$) or after two instances ($p = 0.048$). The difference between one and two instances was not statistically significant ($p = 0.112$). This graded enhancement in functional connectivity, particularly involving the F3, F4, Fz, and Cz channels, suggests that accumulating negative feedback engages a broader and more tightly synchronized network of frontal-central brain regions.

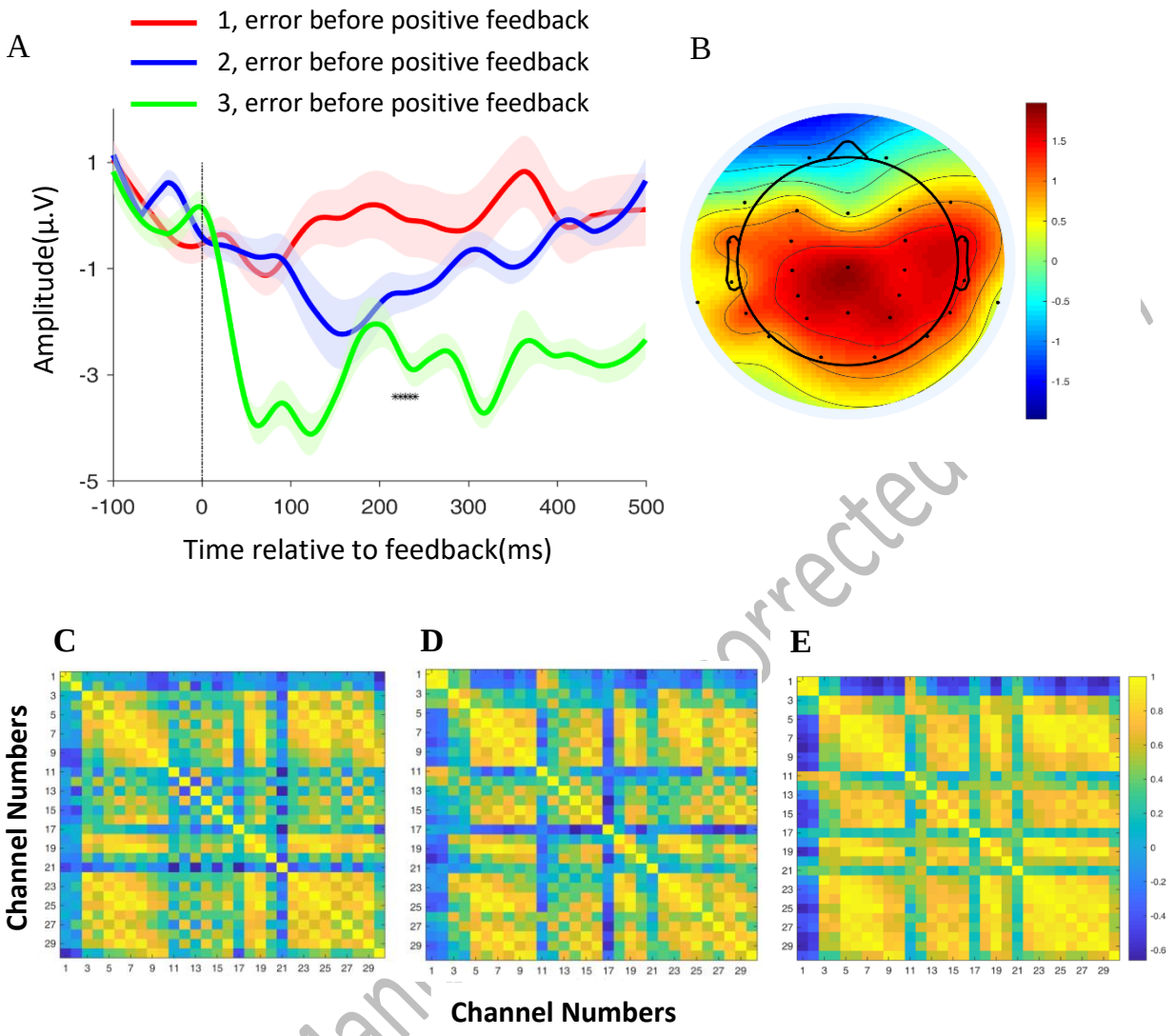

Figure 4. FRN scales with consecutive negative feedback. (A)

FRN amplitude at electrode Fz increases with successive negative feedback (1st, 2nd consecutive, 3rd consecutive) before an environmental change (Kruskal-Wallis test, $p < 0.05$; shading = ±SEM). **(B)** Topographic maps during the FRN peak reveal a strengthening frontocentral negativity (maximal at Fz/Cz) as consecutive negative feedback accumulates. **(C)** Functional connectivity (correlation matrix) following single negative feedback shows baseline coupling within a frontocentral network (Fz–Cz $r = 0.43 \pm 0.09$). **(D)** Connectivity after two consecutive negative feedbacks demonstrates increased synchronization (Fz–Cz, $r = 0.49 \pm 0.15$). **(E)** Three consecutive negative feedbacks elicit peak network integration (Fz–Cz, r =

0.58 ± 0.16). Connectivity after three errors was significantly stronger than after one ($p = .035$) or two ($p = .048$) errors, indicating that accumulating evidence for a strategy failure engages a more coherent frontocentral decision-monitoring network.

FRN Amplitude Scales with Decision Urgency

To investigate whether the FRN component encodes decision urgency during periods of environmental stability, we analyzed neural activity in trials preceding voluntary strategy switches. Based on evidence that switch rates increase with elapsed time in an unchanged environment (Purcell and Kiani, 2016a)—a behavioral marker of rising decision urgency and that FRN amplitude is modulated by adaptive processes (Miletić, 2016), we hypothesized that FRN amplitude would increase systematically as urgency built before a strategic change.

We analyzed FRN signals from trials preceding environmental switches. Trials were categorized into three groups based on their temporal distance from the switch trial. The environment remained unchanged during these pre-switch trials. The first category included trials immediately preceding the switch (1–3 trials before), the second category included trials with intermediate distance (4–6 trials before), and the third category included trials furthest from the switch (7–9 trials before). This classification allowed us to track the evolution of neural activity as participants approached a point of strategic adaptation.

Statistical analysis revealed a significant main effect of temporal proximity on FRN amplitude (Figure 5A; Kruskal-Wallis test: $p < 0.046$ after FDR correction). Post-hoc comparisons using Dunn's test with FDR correction showed that FRN amplitude in the immediate pre-switch condition was significantly larger than in the distant condition ($p < 0.038$). The differences between immediate and intermediate conditions ($p < 0.062$) and between intermediate and distant conditions ($p < 0.104$) did not reach statistical significance after correction. Mean FRN amplitudes

(±SEM) at the Fz electrode were as follows: distant condition: r= -1.9 ± 0.5 μV; intermediate condition: r=-2.1 ± 0.6 μV; immediate pre-switch condition: r=-2.6 ± 0.7 μV.

Scalp topography during the peak FRN interval (300–400 ms post-feedback) displayed a focal frontal-central distribution across all urgency conditions, with maximal negativity consistently observed at the Fz and Cz electrodes (Figure 5B). This pattern aligns with the established neural generators of the FRN in the medial frontal cortex.

We further examined whether increasing decision urgency strengthened functional coupling within the frontal-central network. Correlation-based connectivity analysis was performed on EEG signals from the post-feedback window. The resulting connectivity matrices (Figure 5C, D, E) demonstrated a systematic increase in correlation strength as trials approached the switch point. Specifically, the Pearson correlation coefficient between the Fz and Cz electrodes increased progressively across conditions: distant: 0.36 ± 0.10; intermediate: 0.42 ± 0.11; immediate pre-switch: 0.49 ± 0.12.

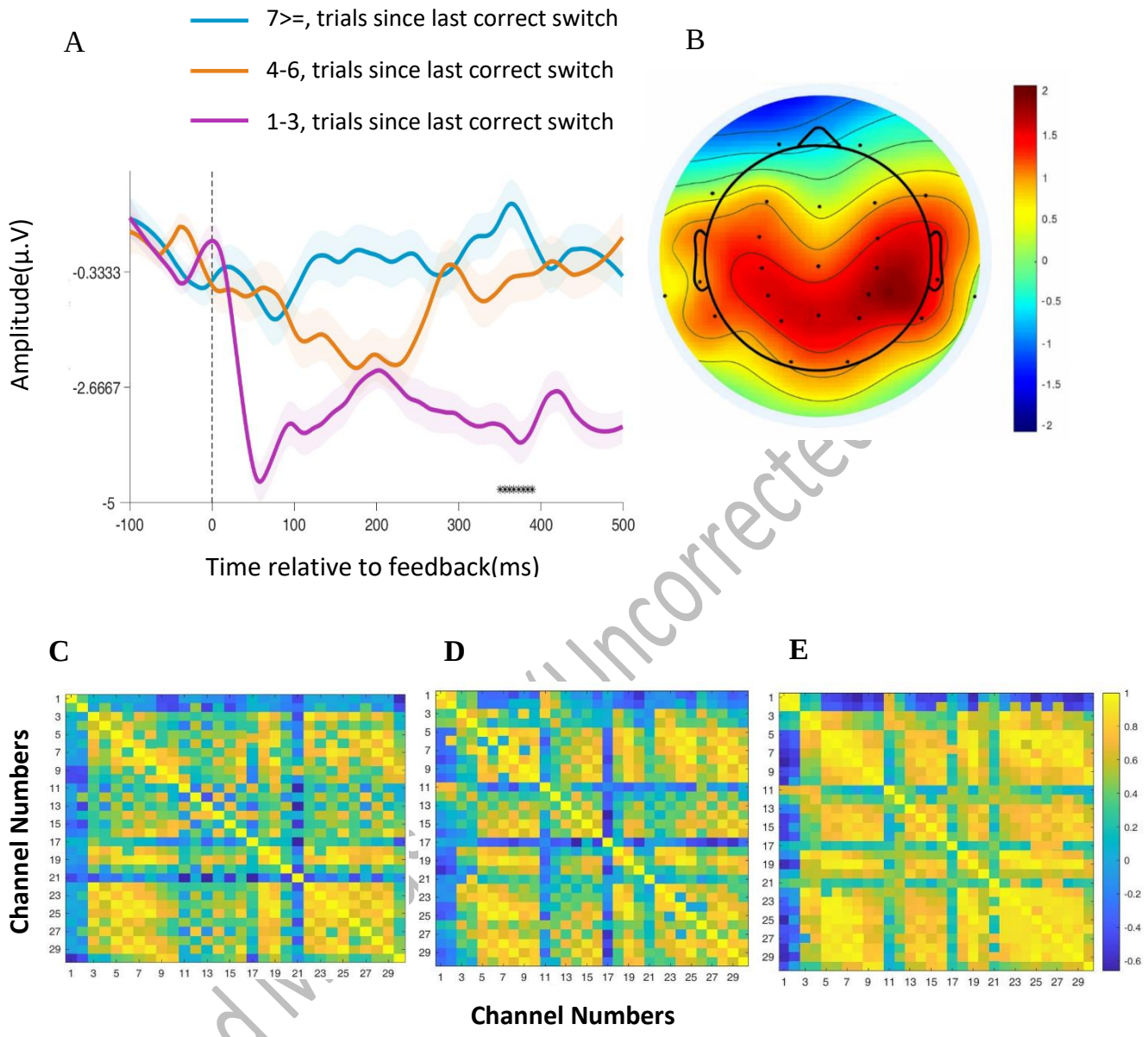

Figure 5: FRN amplitude scales with decision urgency prior to environmental switch. (A) Grand-average waveforms at Fz show progressive enhancement of FRN amplitude as trials approach the switch point, with a significant main effect of temporal proximity (Kruskal-Wallis, $p<0.046$ after FDR correction). Shading indicates SEM. **(B)** Scalp topography during the FRN peak interval shows characteristic frontal-central negativity maximal at Fz and Cz electrodes across all urgency conditions. **(C)** Functional connectivity analysis under low decision urgency (distant trials, 7-9 trials before switch) reveals

baseline frontal-central connectivity patterns. **(D)** Functional connectivity analysis under moderate decision urgency (intermediate trials, 4-6 trials before switch) shows strengthened frontal-central network synchronization. **(E)** Functional connectivity analysis under high decision urgency (immediate pre-switch trials, 1-3 trials before switch) demonstrates maximal network engagement with strongest correlations. Connectivity matrices (Pearson correlation) display correlation strength between EEG channels (self-correlations excluded), with Fz-Cz correlations increasing from 0.36±0.10 (distant) to 0.42±0.11 (intermediate) and 0.49±0.12 (immediate pre-switch).

FRN Amplitude Predicts and Scales with Strategy Change

Consistent with established literature indicating that FRN is amplified in unpredictable task contexts (Pfabigan et al., 2015), we observed a distinct enhancement of the negative wave immediately preceding environmental switches. Specifically, FRN amplitude was significantly larger before compared to after a switch (Figure 6A; Wilcoxon signed-rank $p < 0.05$), suggesting a proactive neural response associated with the anticipation and preparation for strategic adaptation.

This pre-switch FRN intensification likely reflects heightened error-monitoring activity and increased cognitive effort dedicated to evaluating ongoing performance and initiating corrective behavioral change. The topographic distribution of this enhanced negativity was centered over frontal-central regions, with maximal amplitude at Fz and Cz electrodes (Figure 6B), implicating the medial frontal cortex in this preparatory process.

Supporting this interpretation, functional connectivity analysis revealed significantly stronger correlations within a frontal-central network (F3, F4, Fz, Cz) during pre-switch trials compared to post-switch trials (Figure 6C, D). The mean connectivity strength among these key electrodes was

0.53 ± 0.08 in pre-switch trials versus 0.39 ± 0.07 in switch trials (T- test: $p = 0.034$), indicating more synchronized activity within this network prior to strategic change.

In summary, the convergence of amplitude, topography, and connectivity data demonstrates that FRN modulation serves as a predictive neural signal of impending strategy shifts. The component's sensitivity to the pre-switch context underscores its role not merely as a feedback evaluator, but as an integral part of a proactive system that monitors decision efficacy and mobilizes adaptive resources in anticipation of necessary behavioral change within hierarchical decision-making frameworks.

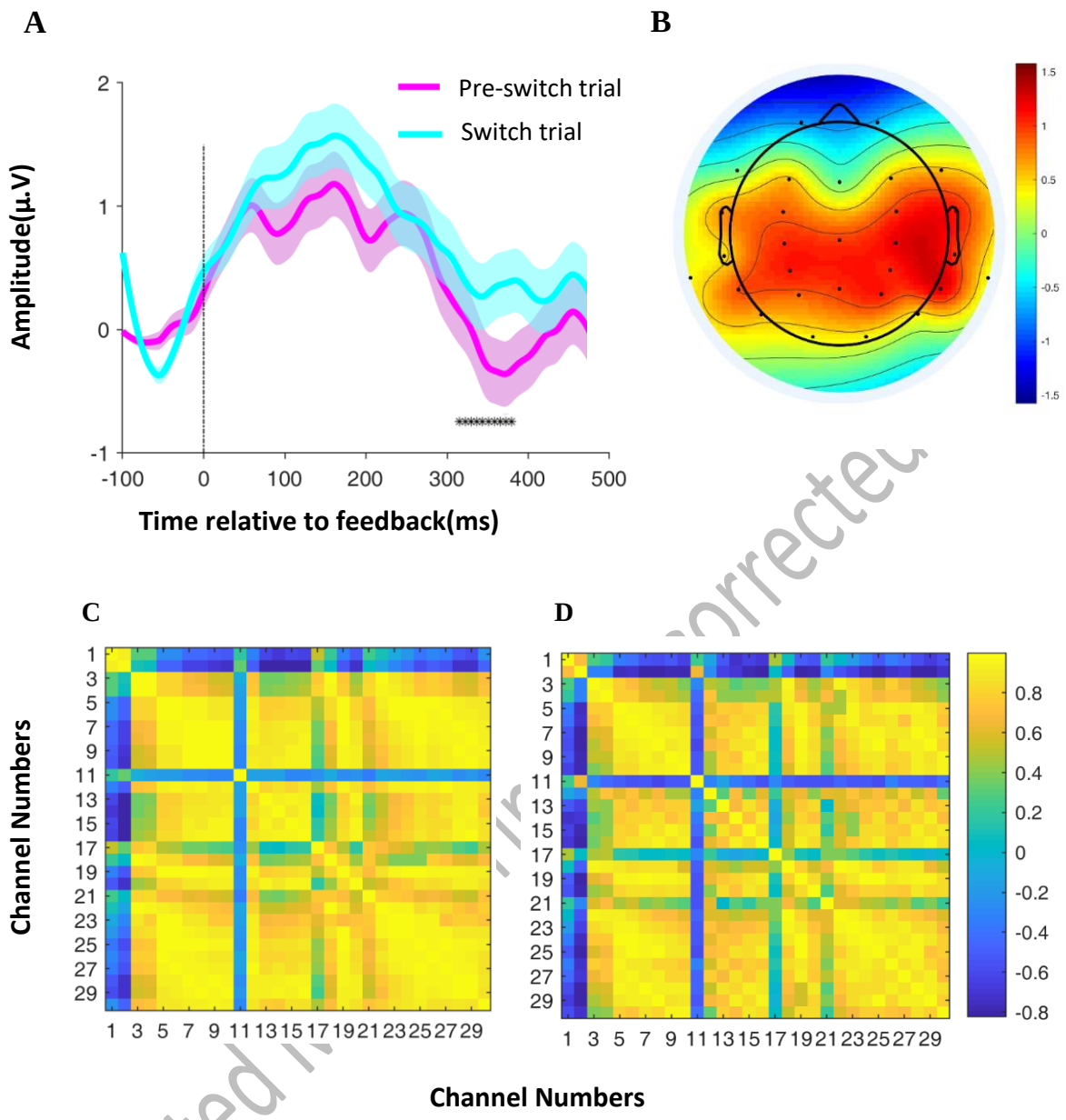

Figure 6: FRN predicts strategy change and signals adaptive preparation. (A) FRN amplitude at Fz is significantly larger before compared to after environmental switching (Wilcoxon signed-rank test, $p<0.05$), suggesting proactive preparation for strategy change. Shading indicates SEM. **(B)** Topographic map during the pre-switch FRN interval shows maximal negativity at frontal-central sites (Fz, Cz), implicating medial frontal cortex in preparatory

processing. **(C)** Connectivity matrix for pre-switch trials reveals strong frontal-central network correlations (mean connectivity: 0.53 ± 0.08). **(D)** Connectivity matrix for switch trials shows reduced correlation strength in the same network (0.39 ± 0.07). Both axes represent EEG channels; color intensity indicates correlation magnitude (self-correlations excluded). These results demonstrate that FRN modulation and associated network synchronization serve as predictive neural signals of impending strategy shifts.

DISCUSSION

The present study provides a detailed examination of the Feedback-Related Negativity (FRN) as a neural correlate of hierarchical decision-making in humans, integrating behavioral and electrophysiological evidence within a single experimental framework. Behavioral analyses showed that negative feedback—particularly when weighted by low-level decision certainty and accumulated across consecutive trials—increases the likelihood of high-level strategy switching (Figure 1E–G). These findings underscore the need for active inference to disambiguate the source of negative outcomes, whether arising from inappropriate high-level strategies or unreliable low-level decision execution. However, behavioral measures alone were insufficient to reliably predict the timing of strategy switches, motivating the investigation of neural signals that may reflect latent evaluative processes preceding overt behavioral change.

FRN analyses yielded three main findings. First, FRN amplitude increased systematically with consecutive negative feedback (Figure 2A), indicating sensitivity to the accumulation of evidence signaling potential strategy failure. Second, FRN enhancement was most pronounced immediately prior to high-level strategy switches (Figure 4A), suggesting that this signal reflects internal evaluative processes that precede explicit behavioral updating. Third, FRN modulation scaled with

stimulus strength and decision urgency (Figure 3B, 4B), consistent with the integration of low-level decision certainty and higher-order contextual variables. Together, these results suggest that the FRN reflects hierarchical evidence integration processes rather than encoding feedback valence alone.

Importantly, FRN dynamics provided information beyond behavior alone. While behavioral measures capture the outcome of decision processes, FRN fluctuations tracked trial-by-trial changes in internal belief updating that preceded observable strategy switches. In this sense, the FRN appears closely related to a latent decision variable reflecting the accumulation of negative evidence toward a strategy-switch threshold, consistent with computational models of hierarchical decision-making. It is important to note that FRN analyses were primarily restricted to negative feedback trials, in line with the evaluative nature of this component. While urgency-related behavioral analyses incorporated both positive and negative feedback to capture overall decision dynamics, interpretations of FRN modulations are confined to evaluative contexts following negative feedback.

The FRN exhibited a consistent frontocentral scalp distribution, in agreement with prior studies linking this component to medial frontal control networks (San Martín, 2012; Shahnazian et al., 2018). The present study did not aim to perform precise neuroanatomical localization, and inferences regarding neural generators should be interpreted as indirect and model-based, given the spatial limitations of scalp EEG. Nevertheless, the observed temporal dynamics, feedback sensitivity, and topographic consistency of the FRN align with the established role of the medial prefrontal cortex (mPFC), particularly the anterior cingulate cortex (ACC), in performance monitoring and adaptive control (San Martín, 2012; McLoughlin et al., 2022).

These findings converge with neurophysiological evidence from non-human primates. Sarafyazd and Jazayeri (2019) demonstrated that neurons in the mPFC, especially within the ACC, integrate low-level decision confidence and accumulated negative feedback to trigger high-level strategy switches once a threshold is reached. Although our EEG data cannot localize activity to the ACC with certainty, the correspondence between the computational variables reflected in human FRN dynamics and those encoded by primate ACC neurons suggests a shared functional architecture underlying hierarchical decision-making across species.

Rather than providing direct evidence for ACC involvement, we propose that the FRN serves as a temporally precise electrophysiological signature of hierarchical evidence integration processes that are known, from invasive recordings, to engage medial frontal circuits including the ACC (Shahnazian et al., 2018; Sarafyazd & Jazayeri, 2019). This interpretation is further supported by human neuroimaging and source-localization studies implicating the ACC in feedback processing and adaptive decision-making (Gluth et al., 2013; Pezzetta et al., 2022), while remaining appropriately constrained by the limitations of EEG.

In summary, this study advances our understanding of hierarchical decision-making by demonstrating that FRN dynamics track the integration of feedback history, decision certainty, and urgency within a unified task. By linking human electrophysiological signals with computational and neurophysiological findings from primates, our results position the FRN as a cross-species neural marker of adaptive strategy updating under uncertainty. Future studies combining hierarchical decision-making paradigms with source-localized EEG, fMRI, or intracranial recordings will be essential to directly test the specific contributions of ACC and related medial frontal networks in humans.

CONCLUSION

In conclusion, the present study demonstrates that the Feedback-Related Negativity (FRN) reflects more than a simple evaluation of feedback valence, serving instead as a neural signature of hierarchical evidence integration during adaptive decision-making. Across a unified task, FRN amplitude systematically tracked the accumulation of negative feedback, sensitivity to low-level decision certainty, and rising decision urgency preceding strategic shifts. Critically, FRN enhancement reliably preceded high-level strategy changes, indicating that this signal captures latent evaluative processes that unfold before overt behavioral adaptation.

These findings position the FRN as a temporally precise marker of hierarchical decision dynamics, linking sensory confidence, feedback history, and urgency into a single neural measure. While scalp EEG does not allow for definitive source localization, the observed frontocentral topography and functional connectivity patterns are consistent with the involvement of medial frontal control networks, including regions such as the anterior cingulate cortex, previously implicated in adaptive control and hierarchical reasoning.

By bridging human electrophysiological evidence with computational and neurophysiological findings from non-human primates, this work supports the view that hierarchical decision-making relies on conserved neural mechanisms across species. Future studies combining hierarchical paradigms with source-localized EEG, fMRI, intracranial recordings, and computational modeling will be essential for directly characterizing the specific neural circuits underlying these adaptive processes and for refining mechanistic accounts of strategy updating under uncertainty.

Ethical Approval

Ethical Committee Approval Number: IR.IUMS.REC.1399.108

ACKNOWLEDGMENTS

This work has partially been supported by the Cognitive Sciences and Technologies Council, and Shahid Rajaee Teacher Training University. We are thankful to Jamal Esmaily Sadrabadi for his helpful discussions.

Data availability

Data will be made available on request for a Corresponding Author.

REFERENCES

Azizi, Z. and Ebrahimpour, R., 2023. Explaining Integration of Evidence Separated by Temporal Gaps with Frontoparietal Circuit Models. *Neuroscience*, *509*, pp.74-95. DOI: 10.1016/j.neuroscience.2022.12.024

Barzegaran, E. and Knyazeva, M.G., 2017. Functional connectivity analysis in EEG source space: the choice of method. *PLoS One*, *12*(7), p.e0181105. DOI: 10.1371/journal.pone.0181105

Beyeler, M., Richert, M., Dutt, N.D. and Krichmar, J.L., 2014. Efficient spiking neural network model of pattern motion selectivity in visual cortex. *Neuroinformatics*, *12*, pp.435-454. DOI: 10.1007/s12021-014-9218-x

Boldt, A. and Yeung, N., 2015. Shared neural markers of decision confidence and error detection. *Journal of Neuroscience*, *35*(8), pp.3478-3484. DOI: 10.1523/JNEUROSCI.4676-14.2015

Britten, K.H., Shadlen, M.N., Newsome, W.T. and Movshon, J.A., 1992. The analysis of visual motion: a comparison of neuronal and psychophysical performance. *Journal of Neuroscience*, *12*(12), pp.4745-4765. DOI: 10.1523/JNEUROSCI.12-12-4745.1992

Daglarli, E., 2020. Computational modeling of prefrontal cortex for meta-cognition of a humanoid robot. *IEEE Access*, *8*, pp.98491-98507. DOI: 10.1109/ACCESS.2020.3000574

García-Hernández, J.P., Iribe-Burgos, F.A., Cortes, P.M., Sotelo-Tapia, C., Guevara, M.A. and Hernández-González, M., 2022. Cortical functionality during reversal learning on a decision-making task in young men. *Brain Research*, *1791*, p.147998. DOI: 10.1016/j.brainres.2022.147998

Ghaderi-Kangavari, A., Parand, K., Ebrahimpour, R., Nunez, M.D. and Amani Rad, J., 2023. How spatial attention affects the decision process: looking through the lens of Bayesian hierarchical diffusion model & EEG analysis. Journal of Cognitive Psychology, 35(4), pp.456-479. DOI: 10.1080/20445911.2022.2088488

Gluth, S., Rieskamp, J. and Büchel, C., 2014. Neural evidence for adaptive strategy selection in value-based decision-making. *Cerebral Cortex*, *24*(8), pp.2009-2021. DOI: 10.1093/cercor/bht049

Gupta, R. and Deák, G.O., 2015. Disarming smiles: irrelevant happy faces slow post-error responses. *Cognitive processing*, *16*, pp.427-434. DOI: 10.1007/s10339-015-0690-0

Holroyd, C.B. and Coles, M.G., 2002. The neural basis of human error processing: reinforcement learning, dopamine, and the error-related negativity. *Psychological review*, *109*(4), p.679. DOI: 10.1037/0033-295X.109.4.679

Iribe-Burgos, F.A., Cortes, P.M., García-Hernández, J.P., Sotelo-Tapia, C., Hernández-González, M. and Guevara, M.A., 2022. Effect of reward and punishment on no-risk decision-making in young men: an EEG study. *Brain Research*, *1779*, p.147788. DOI: 10.1016/j.brainres.2022.1477881

Kelly, S.P. and O'Connell, R.G., 2013. Internal and external influences on the rate of sensory evidence accumulation in the human brain. *Journal of Neuroscience*, *33*(50), pp.19434-19441. DOI: 10.1523/JNEUROSCI.3355-13.2013

Kiani, R. and Shadlen, M.N., 2009. Representation of confidence associated with a decision by neurons in the parietal cortex. *Science*, *324*(5928), pp.759-764. DOI: 10.1126/science.1169405

Knudsen, T., Marchiori, D. and Warglien, M., 2018. Hierarchical decision-making produces persistent differences in learning performance. *Scientific Reports*, *8*(1), DOI: p.15782. 10.1038/s41598-018-34128-w

Li, H. and Zhou, N., 2017. Factors Research on EEG Signal Analysis of the Willingness of Error Reporting. In *Engineering Psychology and Cognitive Ergonomics: Performance, Emotion and Situation Awareness: 14th International Conference, EPCE 2017, Held as Part of HCI International 2017, Vancouver, BC, Canada, July 9-14, 2017, Proceedings, Part I 14* (pp. 141-154). Springer International Publishing. DOI: 10.1007/978-3-319-58941-9_13

Lim, S.H., Nisar, H., Thee, K.W. and Yap, V.V., 2018. A novel method for tracking and analysis of EEG activation across brain lobes. *Biomedical Signal Processing and Control*, *40*, pp.488-504. DOI: 10.1016/j.bspc.2018.01.021

McCracken, H.S., Murphy, B.A., Burkitt, J.J., Glazebrook, C.M. and Yielder, P.C., 2020. Audiovisual multisensory processing in young adults with attention-deficit/hyperactivity disorder. *Multisensory Research*, *33*(6), pp.599-623. DOI: 10.1163/22134808-20201307

McLoughlin, G., Gyurkovics, M., Palmer, J. and Makeig, S., 2022. Midfrontal theta activity in psychiatric illness: an index of cognitive vulnerabilities across disorders. *Biological psychiatry*, *91*(2), pp.173-182. DOI: 10.1016/j.biopsych.2021.10.016

Miletić, S. (2016). Neural evidence for a role of urgency in the speed-accuracy trade-off in perceptual decision-making. Journal of Neuroscience, *36*(22), 5909–5910. https://doi.org/10.1523/JNEUROSCI.1185-16.2016

Mognon, A., Jovicich, J., Bruzzone, L. and Buiatti, M., 2011. ADJUST: An automatic EEG artifact detector based on the joint use of spatial and temporal features. *Psychophysiology*, *48*(2), pp.229-240. DOI: 10.1111/j.1469-8986.2010.00825.x

Murphy, P.R., Wilming, N., Hernandez-Bocanegra, D.C., Prat-Ortega, G. and Donner, T.H., 2021. Adaptive circuit dynamics across human cortex during evidence accumulation in changing environments. *Nature neuroscience*, *24*(7), pp.987-997. DOI: 10.1038/s41593-021-00850-3

Newsome, W.T. and Pare, E.B., 1988. A selective impairment of motion perception following lesions of the middle temporal visual area (MT). *Journal of Neuroscience*, *8*(6), pp.2201-2211.

Nieuwenhuis, S., Holroyd, C.B., Mol, N. and Coles, M.G., 2004. Reinforcement-related brain potentials from medial frontal cortex: origins and functional significance. *Neuroscience & Biobehavioral Reviews*, *28*(4), pp.441-448. DOI: 10.1016/j.neubiorev.2004.03.003

Oliveira, F.T.P., 2005. Electrophysiological correlates of performance monitoring and error detection in response to augmented feedback. Palmer, J., Huk, A.C. and Shadlen, M.N., 2005. The effect of stimulus strength on the speed and accuracy of a perceptual decision. *Journal of vision*, *5*(5), pp.1-1.

Parashiva, P.K. and Vinod, A.P., 2021. Single-trial detection of EEG error-related potentials using modified power-law transformation. *Biomedical Signal Processing and Control*, *67*, p.102563. DOI: 10.1016/j.bspc.2021.102563

Peixoto, D., Verhein, J.R., Kiani, R., Kao, J.C., Nuyujukian, P., Chandrasekaran, C., Brown, J., Fong, S., Ryu, S.I., Shenoy, K.V. and Newsome, W.T., 2021. Decoding and perturbing decision states in real time. *Nature*, *591*(7851), pp.604-609. DOI: 10.1038/s41586-021-03495-9

Pezzetta, R., Wokke, M.E., Aglioti, S.M. and Ridderinkhof, K.R., 2022. Doing it wrong: a systematic review on electrocortical and behavioral correlates of error monitoring in patients with neurological disorders. *Neuroscience*, *486*, pp.103-125. DOI: 10.1016/j.neuroscience.2022.03.017

Pfabigan, D.M., Seidel, E.M., Paul, K., Grahl, A., Sailer, U., Lanzenberger, R., Windischberger, C. and Lamm, C., 2015. Context-sensitivity of the feedback-related negativity for zero-value feedback outcomes. *Biological Psychology*, *104*, pp.184-192. DOI: 10.1016/j.biopsycho.2014.11.006

Purcell, B.A. and Kiani, R., 2016. Hierarchical decision processes that operate over distinct timescales underlie choice and changes in strategy. *Proceedings of the national academy of sciences*, *113*(31), pp.E4531-E4540. DOI: 10 10.1073/pnas.1602348113

Purcell, B.A. and Kiani, R., 2016. Neural mechanisms of post-error adjustments of decision policy in parietal cortex. *Neuron*, *89*(3), pp.658-671. DOI: 10.1016/j.neuron.2016.01.030

Quick Jr, R.F., 1974. A vector-magnitude model of contrast detection. *Kybernetik*, *16*(2), pp.65-67. DOI: 10.1007/BF00271628.

Rawls, E., Miskovic, V., Moody, S.N., Lee, Y., Shirtcliff, E.A. and Lamm, C., 2020. Feedback-related negativity and frontal midline theta reflect dissociable processing of reinforcement. *Frontiers in Human Neuroscience*, *13*, p.452. DOI: 10.3389/fnhum.2020.00452

Roitman, J.D. and Shadlen, M.N., 2002. Response of neurons in the lateral intraparietal area during a combined visual discrimination reaction time task. *Journal of neuroscience*, *22*(21), pp.9475-9489. DOI: 10.1523/JNEUROSCI.22-21-09475.2002

Roshan, S.S., Sadeghnejad, N., Sharifiadeh, F. and Ebrahimpour, R., 2024. A Neurocomputational Model of Decision and Confidence in Object Recognition Task. *Neural Networks*, p.106318. DOI: 10.1016/j.neunet.2023.106318

Salami, F., Bozorgi-Amiri, A., Hassan, G.M., Tavakkoli-Moghaddam, R. and Datta, A., 2022. Designing a clinical decision support system for Alzheimer's diagnosis on OASIS-3 data set. *Biomedical Signal Processing and Control*, *74*, p.103527. DOI: 10.1016/j.bspc.2022.103527

San Martín, R., 2012. Event-related potential studies of outcome processing and feedback-guided learning. *Frontiers in human neuroscience*, *6*, p.304. DOI: 10.3389/fnhum.2012.00304

Sarafyazd, M. and Jazayeri, M., 2019. Hierarchical reasoning by neural circuits in the frontal cortex. *Science*, *364*(6441), p.eaav8911. DOI: 10.1126/science.aav8911

Shadlen, M.N. and Newsome, W.T., 2001. Neural basis of a perceptual decision in the parietal cortex (area LIP) of the rhesus monkey. *Journal of neurophysiology*, *86*(4), pp.1916-1936. DOI: 10.1152/jn.2001.86.4.1916

Shahnazian, D., Shulver, K. and Holroyd, C.B., 2018. Electrophysiological responses of medial prefrontal cortex to feedback at different levels of hierarchy. *NeuroImage*, *183*, pp.121-131. DOI:10.1016/j.neuroimage.2018.07.064

Shooshtari, S.V., Sadrabadi, J.E., Azizi, Z. and Ebrahimpour, R., 2019. Confidence representation of perceptual decision by eeg and eye data in a random dot motion task. Neuroscience, 406, pp.510-527. DOI: 10.1016/j.neuroscience.2019.03.015

Valladares, A.A., González, J.G. and Gómez, C.M., 2017. Event related potentials changes associated with the processing of auditory valid and invalid targets as a function of previous trial validity in a Posner's paradigm. *Neuroscience Research*, *115*, pp.37-43. DOI: 10.1016/j.neures.2017.02.007

von Lautz, A., Herding, J. and Blankenburg, F., 2019. Neuronal signatures of a random-dot motion comparison task. *NeuroImage*, *193*, pp.57-66. DOI: 10.1016/j.neuroimage.2019.03.048

Wang, D., Chen, S., Hu, Y., Liu, L. and Wang, H., 2020. Behavior decision of mobile robot with a neurophysiologically motivated reinforcement learning model. *IEEE Transactions on Cognitive and Developmental Systems*, *14*(1), pp.219-233. DOI: 10.1109/TCDS.2019.2929707

Wang, Y., Cheung, H., Yee, L.T.S. and Tse, C.Y., 2020. Feedback-related negativity (FRN) and theta oscillations: Different feedback signals for non-conform and conform decisions. *Biological Psychology*, *153*, p.107880. DOI: 10.1016/j.biopsycho.2020.107880

Xie, H., Mo, L., Li, S., Liang, J., Hu, X. and Zhang, D., 2022. Aberrant social feedback processing and its impact on memory, social evaluation, and decision-making among individuals with depressive symptoms. *Journal of Affective Disorders*, *300*, pp.366-376. DOI: 10.1016/j.jad.2022.03.030

Zhong, N., Chen, T., Zhu, Y., Su, H., Ruan, X., Li, X., Tan, H., Jiang, H., Du, J. and Zhao, M., 2020. Smaller feedback-related negativity (FRN) reflects the risky decision-making deficits of methamphetamine dependent individuals. *Frontiers in psychiatry*, *11*, p.525711. DOI: 10.3389/fpsyt.2020.525711

Zizlsperger, L., Sauvigny, T., Händel, B. and Haarmeier, T., 2014. Cortical representations of confidence in a visual perceptual decision. *Nature communications*, *5*(1), p.3940. DOI: 10.1038/ncomms4940

Zottoli, T.M. and Grose-Fifer, J., 2012. The feedback-related negativity (FRN) in adolescents. *Psychophysiology*, *49*(3), pp.413-420. DOI: 10.1111/j.1469-8986.2011.01278.x

Zylberberg, A., Fetsch, C.R. and Shadlen, M.N., 2016. The influence of evidence volatility on choice, reaction time and confidence in a perceptual decision. *Elife*, *5*, p.e17688. DOI: 10.7554/eLife.17688

Yahyaie, L., Ebrahimpour, R. and Koochari, A., 2024. Pupil Size Variations Reveal Information About Hierarchical Decision-Making Processes. *Cognitive Computation*, pp.1-12. DOI: 10.1007/s12559-023-10067-3